

# Kinetics of Reversible Aggregation of Soft Polymeric Particles in Dilute Dispersion

He Cheng,<sup>†</sup> Chi Wu,<sup>\*,†,‡</sup> and Mitchell A. Winnik<sup>§</sup>

The Open Laboratory of Bond Selective Chemistry, Department of Chemical Physics, University of Science and Technology of China, Hefei, Anhui, China; Department of Chemistry, The Chinese University of Hong Kong, Shatin, N.T., Hong Kong, China; and Department of Chemistry, University of Toronto, Canada M5S 3H6

Received February 25, 2004

Revised Manuscript Received April 14, 2004

## Introduction

The kinetics of colloidal aggregation has attracted much attention for a long time because of its theoretical implication and industrial application. Two distinct extreme regimes, i.e., the diffusion-limited cluster–cluster aggregation (DLCA)<sup>1–3</sup> and the reaction-limited cluster–cluster aggregation (RLCA),<sup>4–6</sup> have been well established. In DLCA, each collision between two approaching clusters or particles leads to an irreversible sticking, resulting in loosely connected hyperbranched clusters with a typical fractal dimension of 1.7–1.8. The average mass of the clusters is a linear function of the aggregation time. In RLCA, only a very small fraction of collisions can result in one sticking. Therefore, one approaching cluster or particle has a much higher chance to interpenetrate the surface of an existing large cluster before it is finally stuck on it, resulting in a more denser cluster with a fractal dimension of 2.0–2.2, depending on its polydispersity. The average mass of the clusters grows exponentially with the aggregation time.

The reversible process of aggregation is fragmentation, which has been much less studied. So far, only a few experimental studies have been reported,<sup>7–17</sup> partially because colloidal aggregation is usually irreversible. Similarly, fragmentation can also be irreversible and reversible. The irreversible model concentrates on the evolution of the size distribution of cluster aggregates during fragmentation,<sup>9–12</sup> while the reversible model simultaneously considers the processes of fragmentation and aggregation,<sup>13,14</sup> a generalized Smoluchowski equation.<sup>15</sup> However, such a reversible model is normally too complicated to yield an analytical solution without some further assumptions.

Argaman and Kaufman<sup>16</sup> showed that the evolution of the number density of the aggregates was governed by a first-order growth and second-order fragmentation kinetics. Experimentally, it is rather difficult to induce the aggregation and fragmentation without a significant alternation of the concentration or ionic strength or pH. Recently, we found that in the presence of Ca<sup>2+</sup> the aggregation and fragmentation of spherical poly(vinyl caprolactam-*co*-sodium acrylate) microgels can be thermally induced and controlled. Such a colloidal dispersion

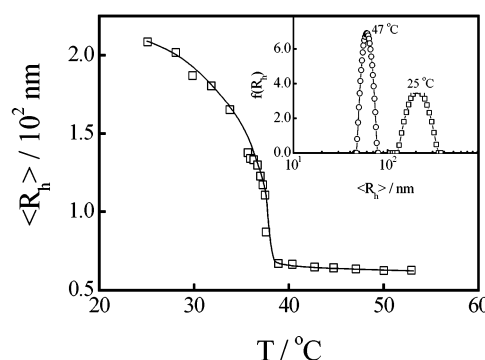


**Figure 1.** Temperature dependence of average hydrodynamic radius  $\langle R_h \rangle$  of spherical microgels in a dilute dispersion ( $2.1 \times 10^{-6}$  g/mL). The inset shows hydrodynamic radius distribution of the microgel at two different temperatures below and higher than the lower critical solution temperature (LCST  $\sim 35$  °C).

provides us a relatively convenient way to attack the existing problem of the reversible aggregation.

## Experimental Section

**Sample Preparation.** Vinyl caprolactam monomer (VCL, courtesy of BASF) was purified by reduced pressure distillation and then recrystallized three times in hexane. Sodium acrylate monomer (NaA, from Aldrich) was used without further purification. Potassium persulfate (KPS, from Aldrich) as initiator and *N,N*-methylenebis(acrylamide) as cross-linking agent (MBAA, from Aldrich) were recrystallized three times in water and methanol, respectively. Calcium chloride (anhydrous CaCl<sub>2</sub>, from ACROS) was used as received. Spherical P(VCL-*co*-NaA) microgels were synthesized by dispersion polymerization. 0.5 g of VCL (93.4 mol %), 14 mg of MBAA (2.4 mol %), 15 mg of SA (4.2 mol %), 5.0 mg of KPS, and 50 mL of deionized water were charged into a polymerization tube. After three freeze–thaw cycles of degassing, the tube was sealed off under vacuum. The reaction was carried at 80 °C for 18 h. The details of the synthesis can be found elsewhere.<sup>18,19</sup> The resultant P(VCL-*co*-NaA) microgels were purified by a successive four cycles of centrifugation (Sigma 2K15 ultracentrifuge, at 15 300 rpm and 40 °C), decantation, and redispersion in deionized water at 25 °C to remove low molar mass molecules.

**Laser Light Scattering.** A commercial LLS spectrometer (ALV/SP-125) equipped with an ALV-5000 multitaue digital time correlator and a He–Ne laser (Uniphase, 22 mW at  $\lambda = 632.8$  nm) was used. In static LLS, the angular dependence of the excess absolute time-averaged scattered intensity, i.e., the Rayleigh ratio  $R_v(q)$ , of a very dilute dispersion can lead to the weight-averaged molar mass  $M_w$  and the  $z$ -averaged root-mean-square radius of gyration  $\langle R_g^2 \rangle_z^{1/2}$  (or written as  $\langle R_g \rangle$ ) of scattering objects,<sup>23</sup> where  $q$  is the scattering vector. In dynamic LLS, the Laplace inversion of each measured intensity–intensity time correlation function  $G^{(2)}(t, q)$  in the self-beating mode can result in a line-width distribution  $G(\Gamma)$ .<sup>23,24</sup> For a pure diffusive relaxation,  $\Gamma$  is related to the translational diffusion coefficient  $D$  by  $(\Gamma/q^2)_{q \rightarrow 0, C \rightarrow 0} = D$  or a hydrodynamic radius  $R_h = k_B T / (6\pi\eta_0 D)$  with  $k_B$ ,  $T$ , and  $\eta_0$  being the Boltzmann constant, the absolute temperature, and solvent viscosity, respectively. The concentration ( $2.6 \times 10^{-6}$  g/mL) of the microgel dispersion used in this study was so dilute that the extrapolation of  $C \rightarrow 0$  was not necessary. The details of LLS instrumentation and theory can be found elsewhere.<sup>23,24</sup>

## Results and Discussion

Figure 1 shows that in pure water without Ca<sup>2+</sup> the microgels shrink from  $\sim 210$  to  $\sim 60$  nm as the temper-

<sup>†</sup> University of Science and Technology of China.

<sup>‡</sup> The Chinese University of Hong Kong.

<sup>§</sup> University of Toronto.

\* To whom correspondence should be addressed at The Chinese University of Hong Kong.

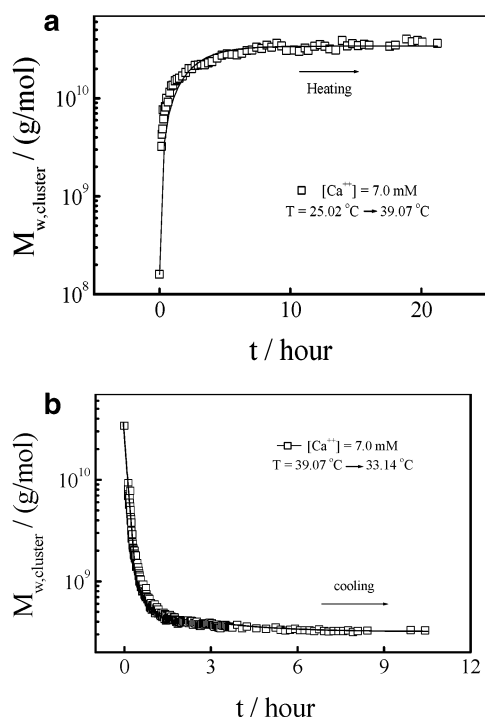


**Figure 2.** (a) After the heating, time dependence of weight-averaged molar mass ( $M_{w,cluster}$ ) of resultant microgel clusters in a dilute dispersion at  $39.07 \pm 0.02$  °C. (b) After the cooling, time dependence of weight-averaged molar mass ( $M_{w,cluster}$ ) of the microgel clusters formed at higher temperatures at  $33.14 \pm 0.02$  °C.

ature increases from 25 to 39 °C, corresponding to a hydrodynamic volume change of  $\sim 40$  times. The inset shows that the microgels are narrowly distributed with a relative width of 0.02. Static LLS results showed that the weight-average molar mass of the microgels was  $1.6 \times 10^8$  g/mol. Note that there was no change in  $M_w$  over the entire temperature range studied; namely, no inter-microgel aggregation without  $\text{Ca}^{2+}$ . It is expected that the microgels used in this study have a “core-shell” structure with the “core” mainly made of cross-linked P(VCL-co-NaA) copolymer chains and a shell which is mainly consisting of hydrophilic NaA groups.<sup>25</sup> This is because at the synthesis temperature (80 °C), PVCL becomes hydrophobic so that longer PVCL segments are in the collapsed state, while short hydrophilic segments containing ionic NaA groups tend to stay on the periphery of the collapsed PVCL “core”. Next, let us examine the situation in the presence of  $\text{Ca}^{2+}$ .

At lower temperatures, long swollen PVCL segments are so hydrophilic that the weak complexation between  $\text{Ca}^{2+}$  and  $\text{COO}^-$  is not able to bring two swollen microgels together. As the temperature increases, the PVCL segments gradually become hydrophobic and phase out in water so that the weak  $\text{Ca}^{2+}/\text{COO}^-$  complexation starts to bind individual microgels together to form large microgel clusters, and the aggregation rate increases with the dispersion temperature. The aggregation is reversible if the temperature is lowered to  $\sim 35$  °C. This enables us to use a simple temperature variation to adjust the rates of aggregation and fragmentation. Figure 2a shows the microgel aggregation at  $T \approx 39$  °C in the presence of  $\text{Ca}^{2+}$ , reflecting in a sharp increase of  $M_{w,c}$ . Note that  $M_{w,c}$  approaches a constant plateau after a long time, suggesting the

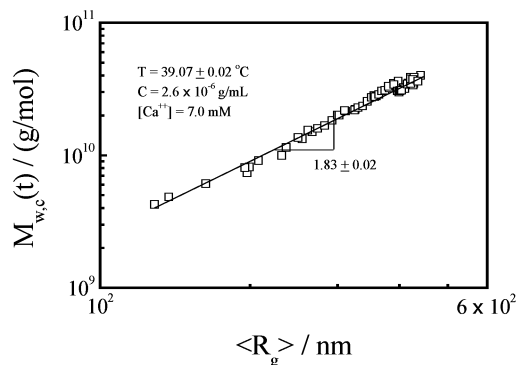


**Figure 3.** Scaling between  $z$ -averaged radius of gyration ( $\langle R_g \rangle$ ) and weight-average molar mass ( $M_{w,c}$ ) of resultant microgel clusters in a dilute dispersion at  $39.07 \pm 0.02$  °C.

formation of stable microgel clusters instead of macroscopic precipitates. We found that the plateau became lower when a lower aggregation temperature was used. This implies the existence of a reversible fragmentation process, whose rate increases as the aggregation proceeds so that a dynamic equilibrium is finally reached. Figure 2b shows that when such a heated dispersion is cooled to low temperatures, the clusters formed at higher temperatures can deaggregate back to individual microgels. Clearly, the aggregation is reversible if the dispersion temperature is sufficiently low.

Figure 3 shows that  $M_{w,c}$  can be scaled to the average radius of gyration ( $\langle R_g \rangle$ ) measured in static LLS, i.e.,  $M_{w,c} \propto \langle R_g \rangle^{1.83 \pm 0.02}$ , suggesting a diffusion-limited cluster-cluster aggregation (DLCA).<sup>1-3</sup> It has been known that DLCA follows a second-order growth kinetics, and the coagulation kernel is independent of the size of resultant aggregates.<sup>20-22</sup> On the other hand, the fragmentation follows first-order kinetics, and its rate is also independent of the size of the aggregates.<sup>20</sup> Assuming that at any given time  $t$   $N(t)$  is the total number of the microgel clusters, including individual microgels in which the aggregation number is only one, we can write the changing rate of  $N(t)$  as

$$\frac{dN(t)}{dt} = -k_a[N(t)]^2 + k_f[N_{\text{microgel}} - N(t)] \quad (1)$$

where  $N_{\text{microgel}}$  is the total molar number of initial PVCL in the dispersion, a constant for a given microgel concentration, and  $k_a$  and  $k_f$  are the rate constants of aggregation and fragmentation, respectively. As  $t \rightarrow \infty$ ,  $dN(t)/dt \rightarrow 0$  for a system at a dynamic equilibrium. In this way, the ratio  $k_a/k_f$  can be solved in terms of  $N(\infty)$  and  $N_{\text{microgel}}$ , i.e.

$$\frac{k_a}{k_f} = \frac{N_{\text{microgel}} - N(\infty)}{N^2(\infty)} \quad (2)$$

Using the two boundary conditions,  $N(0)$  and  $N(\infty)$ , we can analytically solve eq 1 as

$$\ln \frac{[N(t) - N(\infty)][N_{\text{microgel}}N(0) - N(0)N(\infty) + N_{\text{microgel}}N(\infty)]}{[N(0) - N(\infty)][N_{\text{microgel}}N(t) - N(t)N(\infty) + N_{\text{microgel}}N(\infty)]} = -st \quad (3)$$

where  $s = k_f[(2N_{\text{microgel}} - N(\infty))/N(\infty)]$ . Experimentally,  $N(0)$  and  $N(\infty)$  can be determined from the weight-averaged molar masses of the microgel clusters ( $M_{w,c}(0)$  and  $M_{w,c}(\infty)$ ) at  $t \rightarrow 0$  and  $t \rightarrow \infty$ , respectively.

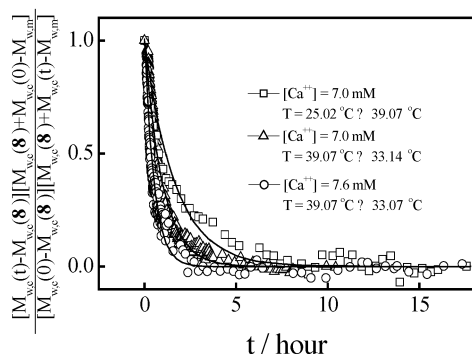


**Figure 4.** Time dependence of function  $\{[M_{w,c}(t) - M_{w,c}(\infty)]/[M_{w,c}(\infty) + M_{w,c}(0) - M_{w,m}]\}/\{[M_{w,c}(0) - M_{w,c}(\infty)][M_{w,c}(\infty) + M_{w,c}(t) - M_{w,m}]\}$  after a microgel dispersion ( $C = 2.6 \times 10^{-6}$  g/mL) was heated or cooled to different temperatures. The solid lines represent the best fittings on the basis of eq 5.

**Table 1. Best Fitting Parameters on the Basis of Eq 5 for Reversible Aggregation of Spherical Poly(vinyl caprolactam-co-sodium acrylate) Microgels in Aqueous Solution ( $C = 2.6 \times 10^{-6}$  g/L) in the Presence of  $\text{Ca}^{2+}$**

$[\text{Ca}^{2+}]$ , mM	$T$ , °C	$M_{w,c}(0)$ , g/mol	$M_{w,c}(\infty)$ , g/mol	$k_a$ , $\text{mol}^{-1} \text{h}^{-1}$	$k_f$ , $\text{h}^{-1}$
7.0	$39.07 \pm 0.02$	$1.6 \times 10^8$	$3.4 \times 10^{10}$	$1.3 \times 10^{15}$	$1.4 \times 10^{-3}$
7.0	$33.14 \pm 0.02$	$3.4 \times 10^{10}$	$3.3 \times 10^8$	$1.3 \times 10^{13}$	$3.3 \times 10^{-1}$
7.6	$33.07 \pm 0.02$	$3.5 \times 10^{10}$	$6.8 \times 10^8$	$8.1 \times 10^{13}$	$2.6 \times 10^{-1}$

This is because the total microgel mass ( $M_{\text{total}}$ ) for a given dispersion is a constant, namely

$$M_{\text{total}} = M_{w,m}N_{\text{microgel}} = M_{w,c}(t)N(t) \quad (4)$$

Since  $N(t)$  is proportional to  $M_{w,c}(t)$ , eq 3 can be rewritten as

$$\frac{[M_{w,c}(t) - M_{w,c}(\infty)][M_{w,c}(\infty) + M_{w,c}(0) - M_{w,m}]}{[M_{w,c}(0) - M_{w,c}(\infty)][M_{w,c}(\infty) + M_{w,c}(t) - M_{w,m}]} = \exp(-st) \quad (5)$$

The left side of eq 5 can be experimentally measured. Figure 4 shows the best fittings of both heating and cooling data on the basis of eq 5. Table 1 summarizes the fitting parameters. As expected, the aggregation dominates the initial process at higher temperatures, but the fragmentation rate gradually increases with time. Note that each cluster, on average, contains  $\sim 230$  microgels when  $t \rightarrow \infty$ . Such an aggregation process is reversible if the temperature is lowered to  $\sim 35$  °C. Note that at lower temperatures each cluster, on average, contains only  $\sim 2$  and  $\sim 4$  microgels, respectively, indicating the microgel clusters formed at higher temperatures are essentially redissolved when the temperature is lower than the LCST. The dynamic equilibrium between aggregation and fragmentation can be better viewed from the ratio of the aggregation rate  $[dN(t)/dt]_a$  and the fragmentation rate  $[dN(t)/dt]_f$ , i.e.

$$-\frac{[dN(t)/dt]_a}{[dN(t)/dt]_f} = \frac{M_{w,c}(\infty)[M_{w,c}(\infty) - M_{w,m}]}{M_{w,c}(t)[M_{w,c}(t) - M_{w,m}]} \quad (6)$$

Figure 5 clearly shows that after the dispersion is cooled the initial process is dominated by the fragmentation, but as the time elapses, the ratio gradually increases and finally approaches one; i.e., the aggregation rate equals the fragmentation rate, at which the dispersion reaches a dynamic equilibrium.

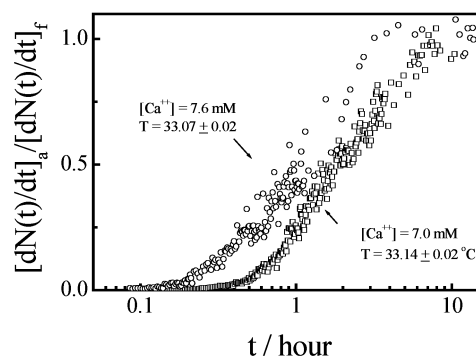


**Figure 5.** Time dependence of rate ratio of aggregation to fragmentation of two different dispersions at two different temperatures.

## Conclusion

The thermally induced aggregation of narrowly distributed spherical poly(vinyl caprolactam-co-sodium acrylate) microgels in the presence of a proper amount of  $\text{Ca}^{2+}$  is a reversible diffusion-limited process with a kinetics consisting of a second-order aggregation and a first-order fragmentation. For a given temperature in the range  $\sim 33$ – $39$  °C, there exists a dynamic equilibrium between aggregation and fragmentation. By varying the dispersion temperature, we can control the rates of aggregation and fragmentation so that the reversible process can be dominated either by aggregation or by fragmentation.

**Acknowledgment.** The financial support of the Hong Kong Special Administration Region Earmarked Grants (CUHK4025/02P, 2160181), the Special Funds for Major State Basic Research Projects (G1999064800), and the CAS Bai Ren Project is gratefully acknowledged.

## References and Notes

- Witten, T. A.; Sander, L. M. *Phys. Rev. Lett.* **1981**, *47*, 1400.
- Witten, T. A.; Sander, L. M. *Phys. Rev. B* **1983**, *27*, 5686.
- Ball, R. C.; Brady, R. M.; Rossi, G.; Thompson, B. R. *Phys. Rev. Lett.* **1985**, *55*, 1406.
- Jullien, R.; Kolb, M. *J. Phys. A* **1984**, *17*, L639.
- Brown, W. D.; Ball, R. C. *J. Phys. A* **1985**, *18*, L517.
- Ball, R. C.; Weitz, D. A.; Witten, T. A.; Leyvraz, F. *Phys. Rev. Lett.* **1987**, *58*, 274.
- McGrady, E. D.; Ziff, R. M. *Phys. Rev. Lett.* **1987**, *58*, 892.
- Botet, R.; Ploszajczak, M. *Phys. Rev. E* **2000**, *62*, 1825.
- Ziff, R. M.; McGrady, E. D. *J. Phys. A: Math. Gen.* **1985**, *18*, 3027.
- Ziff, R. M. *J. Phys. A: Math. Gen.* **1991**, *24*, 2821.
- Ziff, R. M. *J. Phys. A: Math. Gen.* **1992**, *25*, 2569.
- McGrady, E. D.; Ziff, R. M. *Phys. Rev. Lett.* **1987**, *58*, 892.
- Balazs, C.; Hu, J.; Lentovskii, A. P. *Phys. Rev. A* **1990**, *41*, 2109.
- Sintes, T. *Phys. Rev. E* **1994**, *50*, 2967.
- Von Smoluchowski, M. *Phys. Z.* **1916**, *17*, 593.
- Argaman, Y.; Kaufman, W. J.; Sanit, J. *Eng. Div. Am. Soc. Civ. Eng.* **1970**, *96*, 223.
- Vorkapic, D.; Matsoukas, T. *J. Colloid Interface Sci.* **1999**, *214*, 283.
- Peng, S.; Wu, C. *Macromolecules* **2001**, *34*, 6795.
- Peng, S.; Wu, C. *J. Phys. Chem. B* **2001**, *105*, 2331.
- Asnaghi, D.; Carpineti, M.; Giglio, M.; Sozzi, M. *Phys. Rev. A* **1992**, *45*, 1018.
- Fernandez-Barbero; Vincent, B. *Phys. Rev. E* **2000**, *63*, 011509.
- Robinson, D. J.; Earnshaw, J. C. *Phys. Rev. A* **1992**, *46*, 2045.
- Pelton, R. H.; Chibante, P. *Colloids Surf.* **1986**, *20*, 247.
- Wu, C.; Zhou, S. *J. Polym. Phys. Ed.* **1996**, *34*, 1597.
- Daly, E.; Saunders, B. R. *Phys. Chem. Chem. Phys.* **2000**, *2*, 3187.

MA0496201